JOURNAL OF MECHANICAL ENGINEERING AND SCIENCES (JMES)
ISSN: 2289-4659 e-ISSN: 2231-8380
VOL.14, ISSUE 1, 6362 – 6379
DOI: https://doi.org/10.15282/jmes.14.1.2020.13.0498

ORIGINAL ARTICLE

An improved control rod selection algorithm for core power control at TRIGA PUSPATI Reactor

Mohd Sabri Minhat[1,2], Nurul Adilla Mohd Subha[2*], Fazilah Hassan[2] and Norjulia Mohamad Nordin[2]
[1] Reactor Instrumentation and Control Engineering, Reactor Technology Centre, Malaysia Nuclear Agency, Bangi, 43000 Kajang, Selangor, Malaysia.
[2] School of Electrical Engineering, Faculty of Engineering, Universiti Teknologi Malaysia, 81310 Johor Bahru, Johor, Malaysia.
Phone: +60189564289

ABSTRACT – The 1 MWth TRIGA PUSPATI Reactor known as RTP undergoes more than 37 years of operation in Malaysia. The current core power control utilized Feedback Control Algorithm (FCA) and a conventional Control Rod Selection Algorithm (CRSA). However, the current power tracking performance suffers and increase the workload on Control Rod Drive Mechanism (CRDM) if the range between minimum and maximum rod worth value for each control rod has a significant difference. Thus, it is requiring much time to keep the core power stable at the power demand value within the acceptable error bands for the safety requirement of the RTP. In conventional CRSA, regardless of the rod worth value, the lowest position of the control rod is selected for up-movement to regulate the reactor power with 2% chattering error. To improve this method, a new CRSA is introduced named Single Control Absorbing Rod (SCAR). In SCAR, only one rod with highest reactivity worth value will be selected for coast tuning during transient and the lowest reactivity worth value will be selected for fine-tuning rod movement during steady-state. The simulation model of the reactor core is represented based on point kinetics model, thermal-hydraulic models and reactivity model. The conventional CRSA model included with control rod position dynamic model and actual reactivity worth curve data from RTP. The FCA controller is designed based on Proportional-Integral (PI) controller using MATLAB Simulink simulation. The core power control system is represented by the integration of a reactor core model, CRSA model and FCA controller. To manifest the effectiveness of the proposed SCAR algorithm, the results are compared to the conventional CRSA in both simulation and experimentation. Overall, the results shows that the SCAR algorithm offers generally better results than the conventional CRSA with the reduction in rising time up to 44%, workload up to 35%, settling time up to 26% and chattering error up to 18% of the nominal value.

ARTICLE HISTORY
Revised: 9th Dec 2019
Accepted: 9th Dec 2019

KEYWORDS
Control rod selection algorithm;
control rod worth;
core power control;
feedback control algorithm;
TRIGA PUSPATI Reactor.

INTRODUCTION

In nuclear reactor operation, the core power control is a crucial system for a nuclear reactor, which directly affects the safe operation of a nuclear reactor either reactor power or research reactor. For both types of reactors, it is important to ensure that the nuclear reactor is always operated under optimum and safe operating condition [1]. Therefore, continuous research and improvement of the core power control technology for a nuclear reactor is necessary. Among different ways to control the nuclear reaction in fission reactors, the use of control rods can be regarded as the most intuitive. In Training, Research, Isotopes, General Atomics (TRIGA) research reactor, the control rods that containing a solid boron carbide (B_4C) [2] is used to control reactivity during changing in reactor power level and as the main safety mechanism for reactor shut-down. Each control rod is connected to its drive unit called a control rod drive mechanism (CRDM) [3-4]. The CRDM is the hardware unit consists of a motor with reducing gearing a rack-and-pinion to lift (or lowering) the control rods. A potentiometer is connected to the pinion to generate the control rod position indication. As the movement of the control rod at nuclear reactor is mechanically limited, the acceptable ranges for velocity and delay time of the control rod movement must be considered at the design stage [5]. One of the key challenges in core power control is to control the displacement of the control rod accurately using CRDM [6]. In general, the manual controlling system has been used for controlling and tuning control rods in the nuclear reactor by the operator at low power (startup) and automatic controlling system with minimal supervision by operator most of the time at a high-power level for safety purpose.

The TRIGA PUSPATI Reactor (RTP) has four control rods to act as compensating rods. The output signal from the controller will be sent to the control rod selector logic within a control rod speed constraint. The movement of compensating rods is decided by the control rod selector logic [7] known as Control Rod Selection Algorithm (CRSA). To the best of our knowledge, conventional CRSA compensates multiple rods [7] (4 control rods for RTP) or using a single Regulating rod as referring to [8-13] for introducing the external reactivity in TRIGA reactors. The conventional CRSA applied either by getting the minimum position or rod worth value of four control rods and select the lowest value to withdraw the control rod to increase the reactor's power. However, this approach has disadvantage in making the best

*CORRESPONDING AUTHOR | Nurul Adilla Mohd Subha | ✉ nuruladilla@utm.my

© The Authors 2020. Published by Penerbit UMP. This is an open access article under the CC BY license.

decision to control the nuclear reactor based on rod position or rod worth measurement without a systematic approach. After the control rod selection process, the rod will be moved up and down based on the rod drive unit using stepper motor or servomotor.

In general, the rod drive dynamics (control rod position dynamics) is assumed to be ideal which represents by a pure integral function in mathematical form [14-20]. To ensure the rapid process of the rod selection, the conventional CRSA is established by the simplest form of logical sequence control rod movement based on the rod position regardless of the control rod worth value. For instance, simplifying a group of control rods to one control rod [21], taking rod worth curve fitting by using sine wave equation in [22-24], using differential equation based on rod position [25-26], using empirical static function [27], using two control rod model [28] and using control rod withdrawal percentage [7]. Unfortunately, the presented control rod position dynamic model did not consider the actual CDRM and difference between rod worth values for each individual control rods (non-linear function) due to fuel burnup for long time operation in the case of big margin which may lead to inaccuracy result. Moreover, the mismatch CRDM model in design stage may lead to damage of actuator drive due to the high stress of the gearing system (aggressive actuation signal to CRDM) provided by the controller. The work to predict the losses in the gear drive mechanism can be found in [29] which is not considered in this paper.

At RTP, the core power control system uses the Feedback Control Algorithm (FCA) based on the Proportional-Integral (PI) controller to control the reactor core power. According to [30], the controller must be designed to be as simple as possible and easy to be implemented for a nuclear reactor. However, the design process of this common non-model based controller [13] usually not considered the CRSA model which consequently affects the overall tracking performance. Based on previous studies, there is no significant study conducted in investigating the relationship between the power controller and the CRSA. Therefore, in designing the CRSA, the more accurate CRDM or control rod position dynamic model need to be modelled first in the best practice to study the impact on the input actuation signal. After that, the control rod position dynamics model with rod worth values is required to verify the effectiveness of the integration of an improved CRSA for power tracking. The allowable range for power variation in the design criteria must be ±1% (different acceptable range in the case of for PWR-type nuclear reactor up to ±6% [31]) for a nuclear reactor. The rate of power increment limiter must also be considered to avoid the reactor automatic shutdown (Trip). However, this limiter creates unnecessary control rod drive movement which consequently produced undesired power oscillations and longer periods of time to attain power demand [32].

In this study, the mathematical models of the nuclear reactor core in RTP are presented with point-kinetic equations of six-group delayed neutrons, reactivity equations, thermal-hydraulic temperature feedback, FCA controller and CRSA. The MATLAB Simulink used for purpose of controller design and modelled the reactor core before experimental setup [33]. A new CRSA is designed based on the CRDM limits where only one rod can move at one time in practice and consider the difference rod worth values for each individual control rods (reactivity worth curve data). The effectiveness of the proposed CRSA is compared with the conventional CRSA and tested on both numerical simulations and experimentation.

MODELLING OF TRIGA PUSPATI REACTOR

In this section, the mathematical models of the nuclear reactor core in RTP are presented with point-kinetic equations of six delayed neutron precursor groups, thermal-hydraulic equations, fission product poisoning feedback, and reactivity equation.

The dynamic behaviour of the TRIGA nuclear reactor in Figure 1 can be defined by combining the equation of point kinetic, thermal-hydraulic, xenon concentration feedback and reactivity [26]. The equations are defined as follows:

The point kinetic equations of six delayed neutron precursors groups are described in Equation. (1) [15] and [16]:

$$\begin{cases} \dfrac{d\psi}{dt} = \dfrac{\rho - \beta}{\Lambda}\psi + \displaystyle\sum_{i=1}^{6} \lambda_i \eta_i \\ \dfrac{d\eta_i}{dt} = \dfrac{\beta_i}{\Lambda}\psi - \lambda_i \eta_i \quad i = 1, \ldots, 6 \end{cases} \tag{1}$$

where, ψ is relative neutron density, ρ is total reactivity, β is the total fraction of effective delayed neutron, Λ is mean neutron generation time, λ_i is decay constant of the i-th group of delay neutron precursor, η_i is the i-th group of normalized precursor concentration and β_i is the i-th group of delayed neutron.

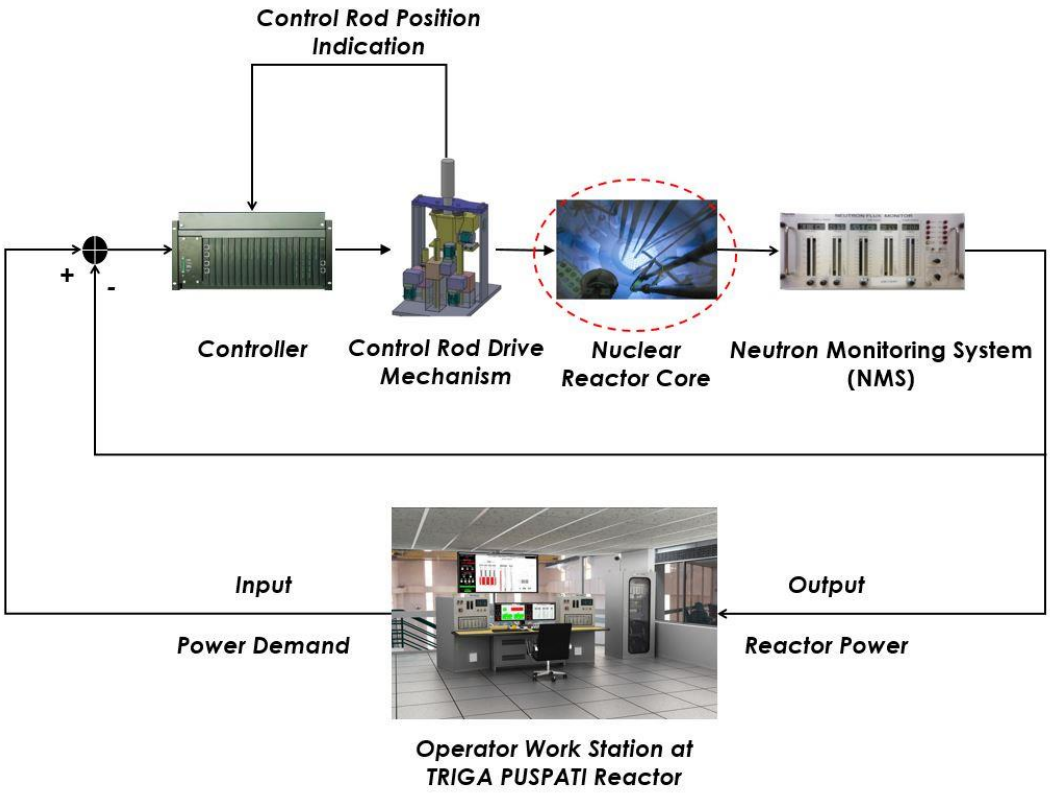

Figure 1. Core power control at RTP.

The thermal-hydraulic Equation. (2) takes into account the behaviour of moderator as a coolant and fuel temperature feedback according to [22], [31] and [34]. In nuclear reactor, the heat exchanger between fuel and coolant moderator within the primary cooling system and the conservation of energy equation between coolant moderator and the secondary cooling system can expressed as:

$$\begin{cases} \dfrac{dT_m}{dt} = \dfrac{P_o(1-f)}{M_m C_m} + \dfrac{T_f - T_m}{M_m C_m / K} - \dfrac{\Gamma}{M_m}(T_m - T_{in}) \\ \dfrac{dT_f}{dt} = \dfrac{P_o f}{M_f C_f} - \dfrac{T_f - T_m}{M_f C_f / K} \\ T_m = wT_{out} + (1-w)T_{in} \\ \Gamma = \dfrac{Kw(T_f - T_m)}{C_m(T_m - T_{in})} \end{cases} \tag{2}$$

where, T_m is average temperature of coolant, P_o is nominal core power, f is fraction of power deposited in the fuel, M_m is moderator total mass, C_m is moderator specific heat capacity, T_f is average temperature of fuel, K is global heat transfer coefficient, Γ is coolant mass flow rate, T_{in} is average inlet temperature of coolant, M_f is fuel total mass, C_f is fuel specific heat capacity, w is weighting factor for computation of moderator temperature, and T_{out} is average outlet temperature of coolant.

In TRIGA type reactors, the average inlet temperature of the coolant is normally constant at about 28°C. So the physical parameter for average of inlet coolant moderator can be initialised to be constant as long as the heat exchanger run during operation.

The effect of fission product poisoning is considered in TRIGA where the xenon concentration feedback can be defined as:

$$\begin{cases} \dfrac{d\delta X}{dt} = \lambda_I \delta I + \left(\gamma_X \sum_f - \sigma_X X_0\right) V \delta\psi - (\sigma_X V \psi_0 + \lambda_X)\delta X \\ \dfrac{d\delta \mathrm{I}}{dt} = \gamma_I \sum_f V \delta\psi - \lambda_I \delta I \end{cases} \tag{3}$$

where, X is the concentration of xenon, λ_I is the decay constant of xenon, I is the concentration of iodine, γ_X is xenon yield per fission, $\sum_f$ is macroscopic fission cross section of fuel, σ_X is microscopic absorption cross section of xenon, X_0 is the concentration of xenon at initial equilibrium state, V is mean velocity of thermal neutron, ψ_0 is relative neutron density at initial equilibrium state, λ_X is the decay constant of xenon, γ_I is iodine yield per fission and λ_I is the decay constant of iodine.

The reactivity equation for TRIGA in Equation. (4) is expressed as the sum of reactivity due to control rod movement, reactivity due to two temperature feedback [19], [34-35], and for long time operation; reactivity due to xenon concentration feedback [36] need to be included.

$$\rho = a_h \Delta h_{cr} + \alpha_m (T_m - T_m^0) + \alpha_f \left(T_f - T_f^0\right) + \sigma_X (X - X_0) \tag{4}$$

0where, a_h is reactivity worth of the control rod, h_{cr} is control rod position, α_m is reactivity due to change in temperature moderator, T_m^0 is the average temperature of moderator at initial equilibrium state, α_f is reactivity due to change in temperature fuel and T_f^0 is average temperature of fuel at initial equilibrium state.

The linearization process of the non-linear dynamic TRIGA model based on Equations. (1-4) using perturbation theory is presented in [37]. In this study, the non-linear equations of the RTP model and all the model parameters with physical quantities of the model parameters can be referred to [38].

FEEDBACK CONTROL ALGORITHM

In this section, the Feedback Control Algorithm (FCA) based on Proportional-Integral (PI) controller is briefly described below.

$$\begin{cases} u_{PI} = G_3 E + G_4 \int_{t_0}^{t} E dt \\ E = \left[G_1 log \left(\dfrac{PDM}{N} \right) \right]_{\pm 1} - G_2 \dfrac{1}{N} \dfrac{dN}{dt} \\ N = \psi P_o \end{cases} \tag{5}$$

The closed-loop of RTP power control system is depicted in Figure 2 [39]. By referring to Figure 2, variable G_1, G_2, G_3 and G_4 act as control gains used to limit the power change rate below 12.5%/s bound, and E is an error deviation (%) which can be expressed as Equation. (5).

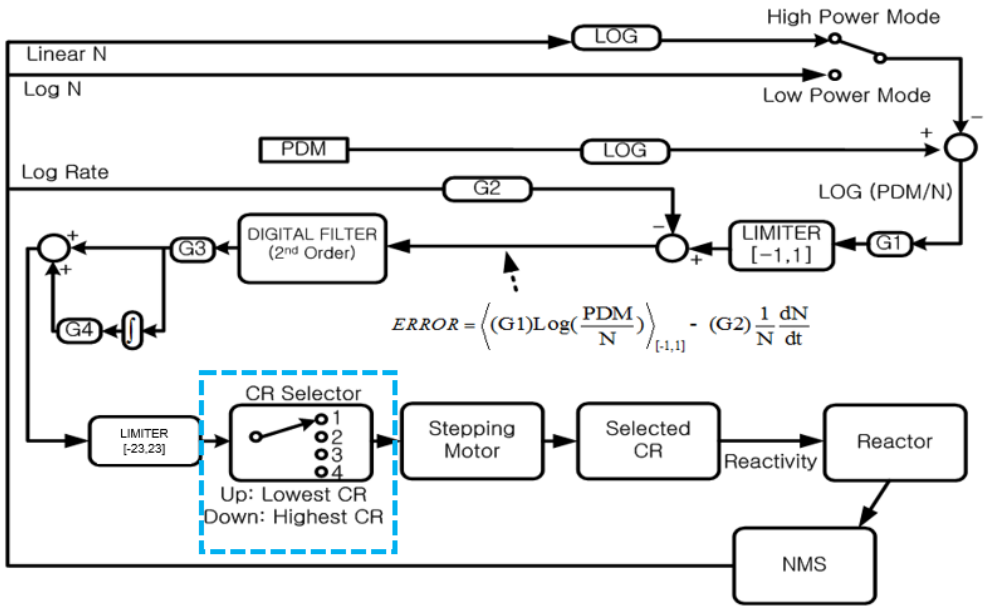

Figure 2. Feedback Control Algorithm (FCA) for automatic control mode.

The FCA controller is designed based on classical control law and to determine the control rod velocity (the motor control command), u_{PI} using error deviation between actual core power, N from Neutron Measurement System (NMS) and power demand (PDM). The detail on FCA designed can be found in [38].

CONTROL ROD SELECTION ALGORITHM (CRSA)

The FCA control performance has been tested at RTP from low power about 1% Full Power (FP) to nominal power operation about 75% FP. The overall power control performance analysis was done by using the gathered operation data from RTP. The steady-state error or noise measure (power fluctuation) after power stable at desired power demand is observed and shown in Figure 3. According to [25], in the presence of switching imperfections, such as switching time delays and small time constants in the actuators, the discontinuity in the feedback control produces a particular dynamic behaviour in the vicinity of the surface, which is commonly referred to as chattering error. This phenomenon is a serious disadvantage (problem) and will produce a high-frequency oscillation of a controlled system, which degrades the performance of the system and may even lead to instability.

Referring to Figure 3, the performance of power control has chattering error (e_{ce}) of 2% of full power [40]. The reactor power tracking performance and chattering error at RTP are the main issues that need to be solved in this research study. For the power control system at RTP, by using the FCA, the control rod speed is limited to ±23 steps per cycle (labelled as *V3*) equivalent to ±2.0355 mm/s as shown in Figure 4.

To date, the CRSA at RTP is the conventional CRSA method where it is applied by getting the minimum position of control rods and select the lowest control rod for up-movement (increase power) or the other way around to regulate reactor power with 2% chattering error. The advantage of this conventional CRSA is to minimize the moving distance of each control rod or known as balancing position control rod method. However, it suffers during transient and fine-tuning in steady-state to regulate reactor power due to differences in control rod worth value for each control rod at RTP and can be found in [41].

The data control rod worth value is very important as a reference for the reactor operator to control the reactivity in the nuclear reactor. The reactor power can be increased by withdrawing the control rods from the reactor core. In conventional CRSA, the lowest position control rod is selected to be withdrawal first regardless of its rod worth value. If the selected control rod at that time is the highest rod worth value, the more positive reactivity will be given to the reactor consequently the more power is produced. More power produced than the demand, the FCA will suffer to correct the error by selecting the highest position of the control rod to be inserted into the core to provide negative reactivity in order to reduce the reactor power. The detail conventional CRSA algorithm at RTP can be found in [26] and the simplified algorithm block diagram shown in Figure 5.

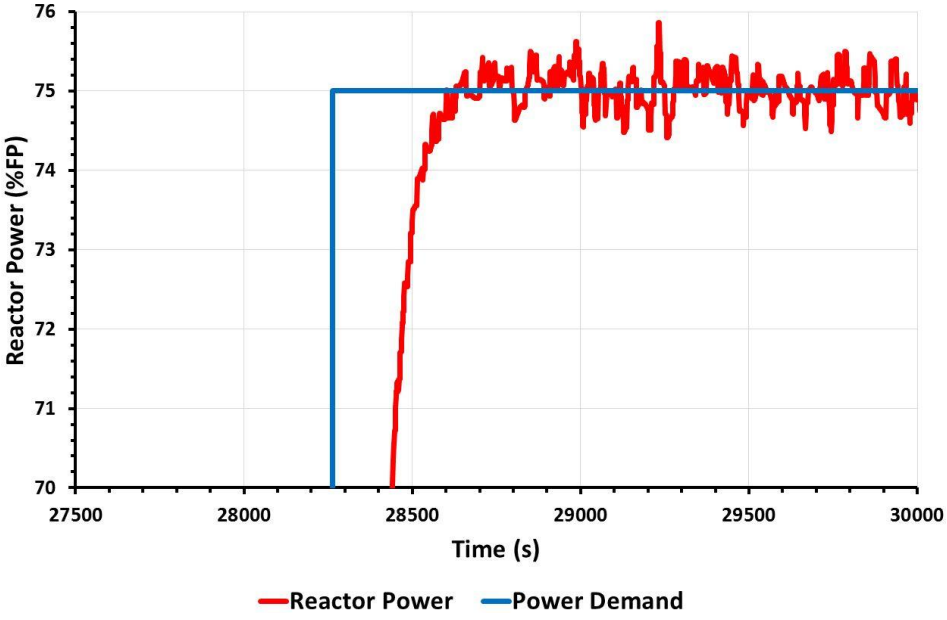

Figure 3. Chattering error (e_{ce}) at 75% full power.

Another type of conventional CRSA method is proposed in [7] for the Egyptian Second Testing Research Reactor (ETRR-2). Instead of taking the lowest rod position to be withdrawal, the control rod with the lowest worth value is selected to increase the reactor power or vice versa. The control rod position of each control rod will be not the same by using this approach (difference rod worth value for each control rod). However, this rod selection strategic will be no guarantee provided the same result in the case of RTP due to a big difference between a minimum and maximum control rod worth value.

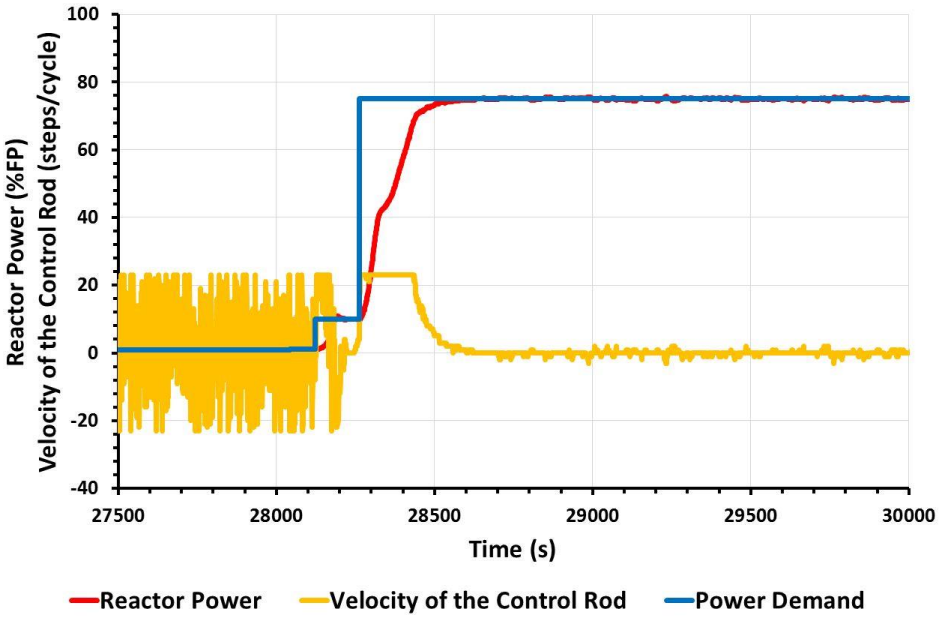

Figure 4. FCA-CRSA performance at RTP.

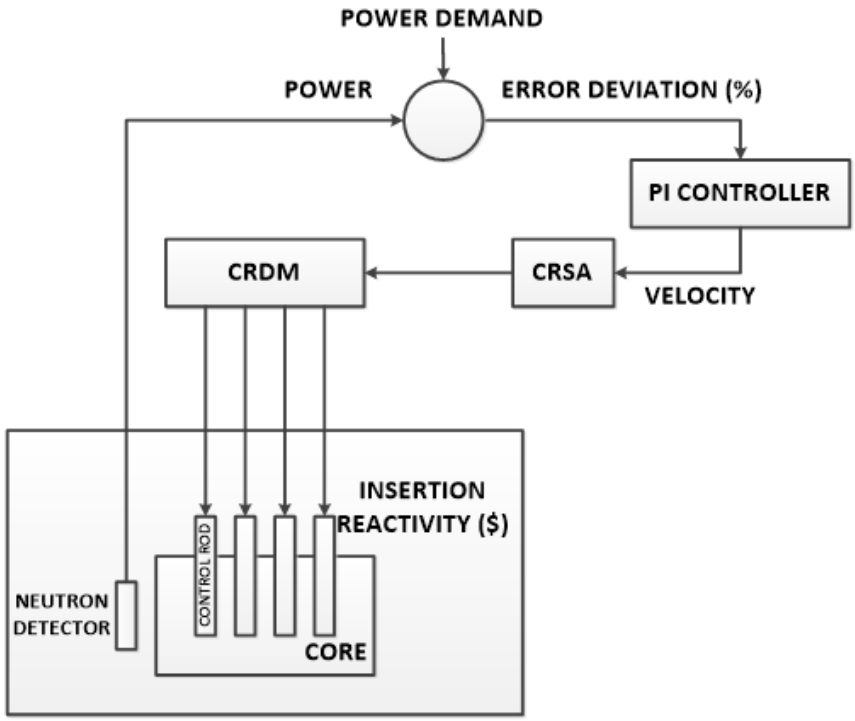

Figure 5. Conventional CRSA algorithm block diagram.

Both conventional CRSA methods (RTP and ETRR-2) have the disadvantage to make the best decision to control power in the nuclear reactor. In addition, the controller action in both methods is solely based on the error equation and the output of the controller (velocity) will be sent to the CRSA system without considering the dynamic control rods behavior. Consequently, it will reduce the tracking performance due to conventional CRSA stick to rely on either rod position or rod worth values to compensate for four control rods.

The conventional CRSA at RTP can be calculated by the following algorithm [42]:

```
// Select Compensating Rod with Minimum Rod Position for Withdrawal
if(SHUTDOWN==F){
  if(Current Control Mode==AUTO){
      if(V3>0){
           num_of_fully_up_CRs=0;
      for(i=1 ; i <5 ; i++){
           if(CR(i)_FULLY_UP==T){num_of_fully_up_CRs++;}
           if( (Carrier Up Switch of CR(i)==F)&&(S(i)==F) ){
              HI_unavailability(i)=F;
           }
           else{
             HI_unavailability(i)=T;
           }
         }
      MIN_POS_COUNTER = min(CR(i)_POSITION_COUNTER+19000*HI_unavailability(i));
      // i=1,..,4
      for(i=1 ; i <5 ; i++){
if( (CR(i)_POSITION_COUNTER<=MIN_POS_COUNTER)&&(HI_unavailability(i)==F) ){
                    CR(i)_selected=T;
                    CR(j)_selected=F; //(j!=i)
                    }
      }
   }
  }
}
// Select Compensating Rod with Maximum Rod Position for Insertion
if(SHUTDOWN==F){
  if(Current Control Mode==AUTO){
     if(V3<=0){
      for(i=1 ; i <5 ; i++){
        if( (Carrier Down Switch of CR(i)==F)&&(S(i)==F) ){
       LOW_availability(i)=T;
       }
         else{
       LOW_availability(i)=F;
       }
       }
MAX_POS_COUNTER=max(CR(i)_POSITION_COUNTER*LOW_availability(i));// i=1,...,4
      for(i=1 ; i <5 ;i++){
           if( (CR(i)_POSITION_COUNTER>=MAX_POS_COUNTER)&&(LOW_availability(i)==T) ){
         CR(i)_selected=T;
         CR(j)_selected=F; //(j!=i)
        }
      }
   }
  }
}
```

Figure 6. Conventional control rod selection algorithm.

The algorithm only limited to control rod selection logic. The algorithm describes in "operating" status (*SHUTDOWN == F*) and current control mode in "automatic", the conventional CRSA define a local variable to save the number of fully up control rods. If a rod is not fully up nor frozen status *S(i)*, then it is declared to be available to move up more.

The *V3* is the number of steps per cycle given by controller. The conventional CRSA get the minimum position of control rods and select the lowest control rod in up-movement (*V3>0*). The other control rods are deselected. The number *19000* indicates 381mm and this big value makes it possible to get rid of an unavailable rod from minimum value calculation.

The algorithm can be operated for the other way around to insert control rod or down-movement (*V3<=0*). The conventional CRSA declares that not fully down and not frozen control rods are available. Then, it will take the maximum value amongst only available control rods and defines the highest position using this value.

A similar algorithm is used by conventional CRSA in [7] with a slightly different local variable name. For example, "*CR(i)_POS_COUNTER*" (rod position) is represented by "*CR(i)_CrWorth*" (rod worth) in [7].

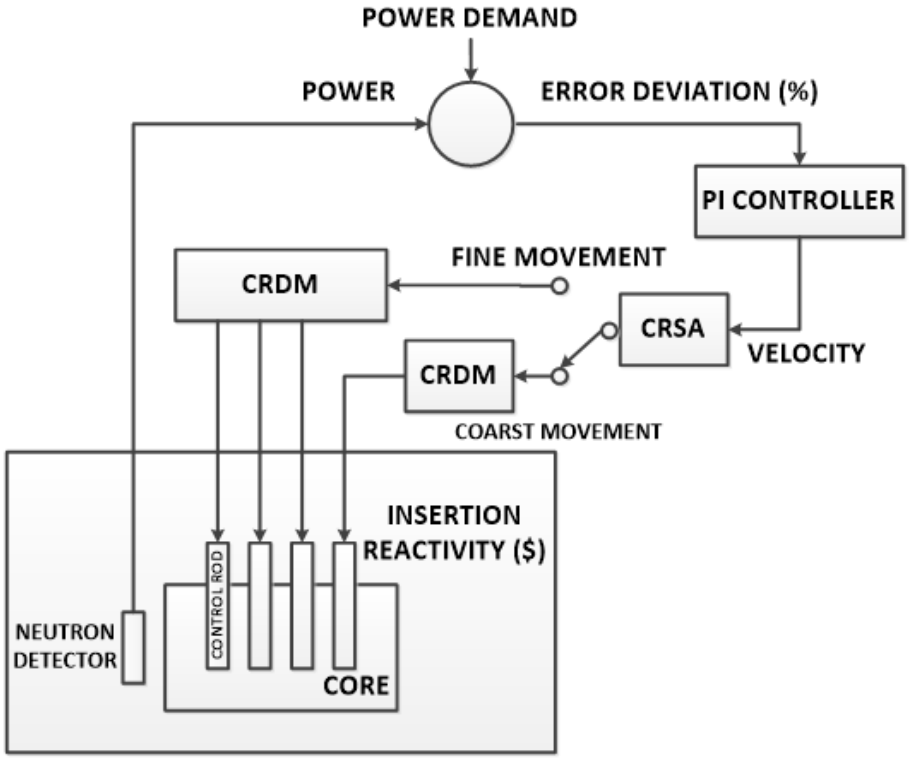

Figure 7. SCAR algorithm block diagram.

The optimal solution with less complexity and time response for the selection rods is introduced in the nuclear reactor. The solution proposed named as a single control absorbing rod (SCAR) and the block diagram is presented in Figure 7. In SCAR, three different approaches are introduced for the three different conditions to achieve the optimum power control performance. During low power condition (subcritical state), only three rods that have the lowest control rod worth available will be selected i.e. Transient (TR) rod, Safety (SF) rod and Shim (SH) rod to reach a critical state. The highest rod worth value Regulating rod (RG) is selected during the transient region to boost up the tracking performance to reach the desired power. At steady-state conditions, the movement of the rod is fine-tuned using the lowest rod worth value.

The SCAR has design restrictions for fine-tuning in the safe mode such as error power control signal (power demand–actual power) within pre-defined value at the steady-state region. This value was introduced in the system to remove unwanted control action consequently reduced fluctuation power error. When the error signal within the pre-defined value, the SCAR will choose the lowest rod worth value to move. Otherwise (not in a steady-state region), the SCAR using select the fast-acting rod (the highest rod worth value) to move. With this proposed approach, the execution time, the possibility of damaging the actuator (workload on CRDM) and the power chattering error can be reduced. The proposed SCAR algorithm is presented in Figure 8:

```
// Single Compensating Rod for Withdrawal
if(SHUTDOWN==F){
  if(Current Control Mode==AUTO){
    if(V3>0 && (|Error Power Control Signal |>= Pre-defined Value)  ){
      for(i=3){
        if( (Carrier Up Switch of CR(i)==F)&&(S(i)==F) ){
              CR(i)_selected=T;
              CR(j)_selected=F; //(j!=i)
        }
             else{
                    CR(i)_selected=F;
                    CR(j)_selected=F; //(j!=i)
              }
        }
           }
 }
}
// Single Compensating Rod for Insertion
if(SHUTDOWN==F){
  if(Current Control Mode==AUTO){
     if(V3<=0 && (|Error Power Control Signal |>= Pre-defined Value)  ){
       for(i=3){
         if( (Carrier Down Switch of CR(i)==F)&&(S(i)==F) ){
              CR(i)_selected=T;
              CR(j)_selected=F; //(j!=i)
          }
         else{
              CR(i)_selected=F;
              CR(j)_selected=F; //(j!=i)
        }
        }
     }
  }
}
```

Figure 8. SCAR algorithm

The initial conditions of SCAR are similar to conventional CRSA which is the status is "operating" and the control mode is "automatic". With SCAR, the number of fully-up control rods and the availability of declared control rods to move up will not be checked. To increase power, only one rod with the highest rod worth value i.e. RG ($i=3$) will be withdrawal. The same approach is used to reduce the reactor power.

EXPERIMENTAL SETUP, RESULTS AND DISCUSSION

In order to enhance the present controller performance, the development of a non-linear dynamic model of the reactor core using Equations. (1-4) with the original controller using Equation. (5) were necessary. The controller gains were set to 12.3, 0.08, 10 and 1e-7 for G_1, G_2, G_3, and G_4, respectively. The simulation model was validated by comparing the experimental data from RTP as depicted in Figure 9. It can be seen that the error between these two results has almost converged to zero at steady-state. The small differences between the simulation and the experimental results are because of the noise and system uncertainty as mention in [29]. However, in this study, the difference is negligible thus indicates that the developed RTP model using a non-linear analytical method can closely represent the actual dynamic of the RTP.

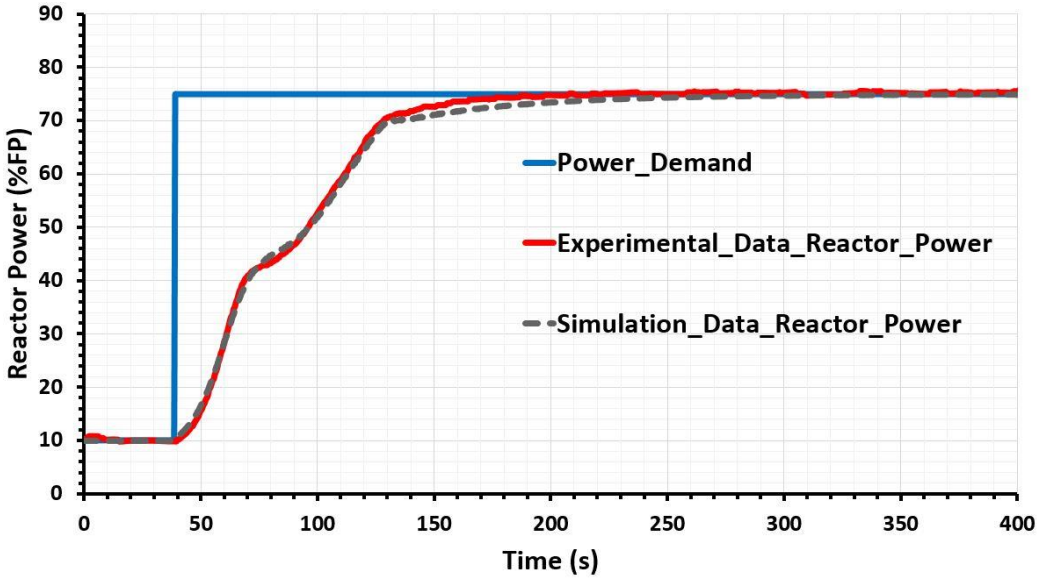

Figure 9. Comparison between experiment data and the model response at 750kWth.

The control rod position dynamic can be represented by the simplest form of control rod position dynamic, i.e. pure integral function. However, this simplicity may lead to inaccuracy results where the difference in control rod worth value for each control rod is ignored. In order to ensure high accuracy in making the decision of rod selection, the control rod position dynamic is derived based on a set of actual input and output data using system identification (System ID) [43]. The comparison between the models is illustrated in Figure 10 and Figure 11. The step input shown in Figure 10 is the constant value of control rod velocity with 2.0355 mm/s (equal to 0.4071 mm/cycle) which is fed to the different types of control rod position dynamics in every 0.2 s/cycle.

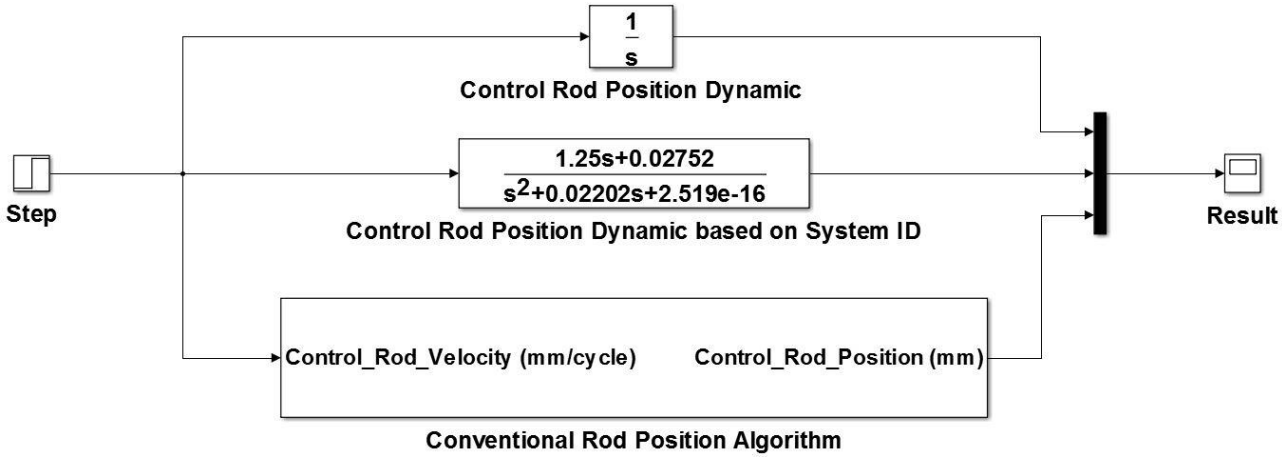

Figure 10. Three different methods to represent the control rod position dynamic.

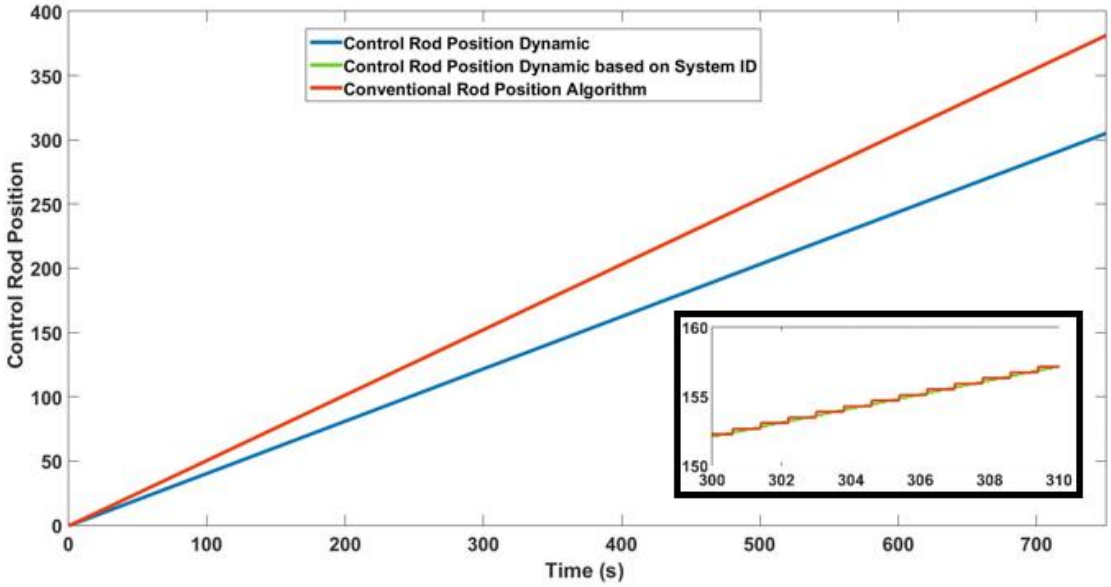

Figure 11. The simulation result of the models in Figure 10.

Referring to Figure 11, the control rod position dynamic based on System ID has 99% best fit thus provide a more accurate model to closely representing the actual rod drive mechanism compare to the pure integral function which has around 80% best fit. The model derived using System ID uses a set of actual input and output data of control rod drive mechanism while the pure integral method does not count the actual data. Thus, the control rod position dynamic based on System ID is more reliable to be implemented in representing the rod drive mechanism in the simulation. This model is then used in obtaining the reactivity worth value.

In order to obtain the reactivity value, the step input shown in Figure 12 is assumed to be the control rod velocity determined by the controller to control the reactivity insertion rate in the reactor core which is Multiple-Inputs-Single-Output (MISO) system [44]. The conventional CRSA and SCAR algorithm will translate the control rod velocity to control rod height parameter (control rod distance travel movement) and assigned as the first input in rod worth curve block. While the initial rod position at initial low power is assigned as the second input. The difference between these two inputs will be converted to rod worth value which indicates the required reactivity insertion from the control rods to increase the reactor power.

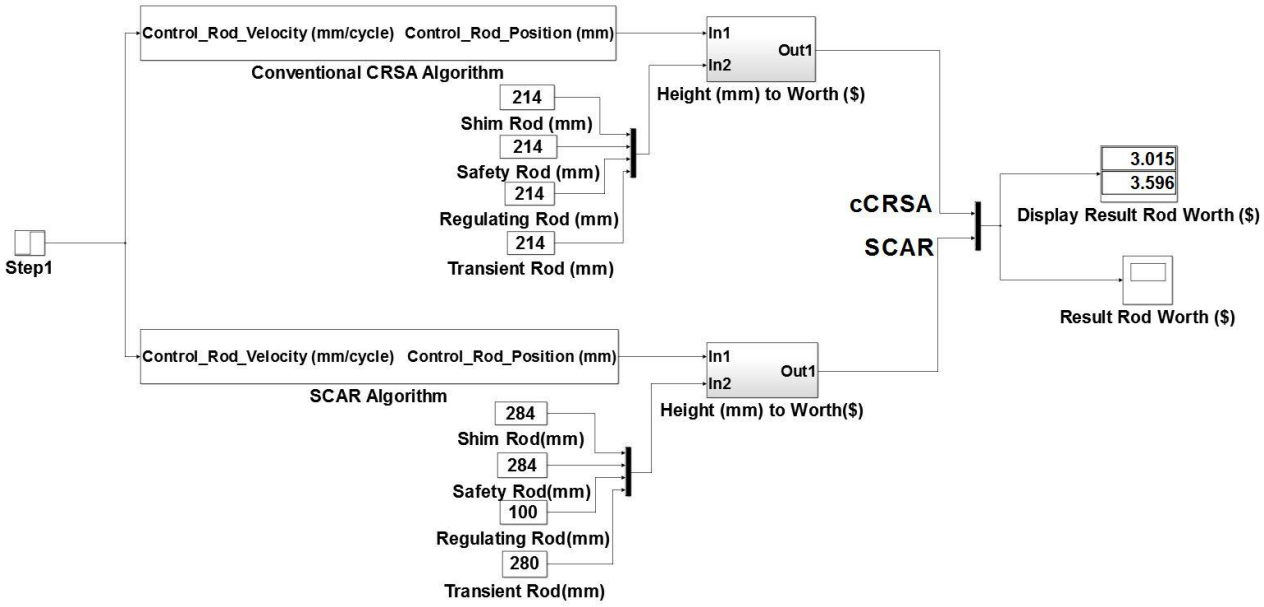

Figure 12. Comparison between conventional CRSA and SCAR in obtaining the reactivity worth value.

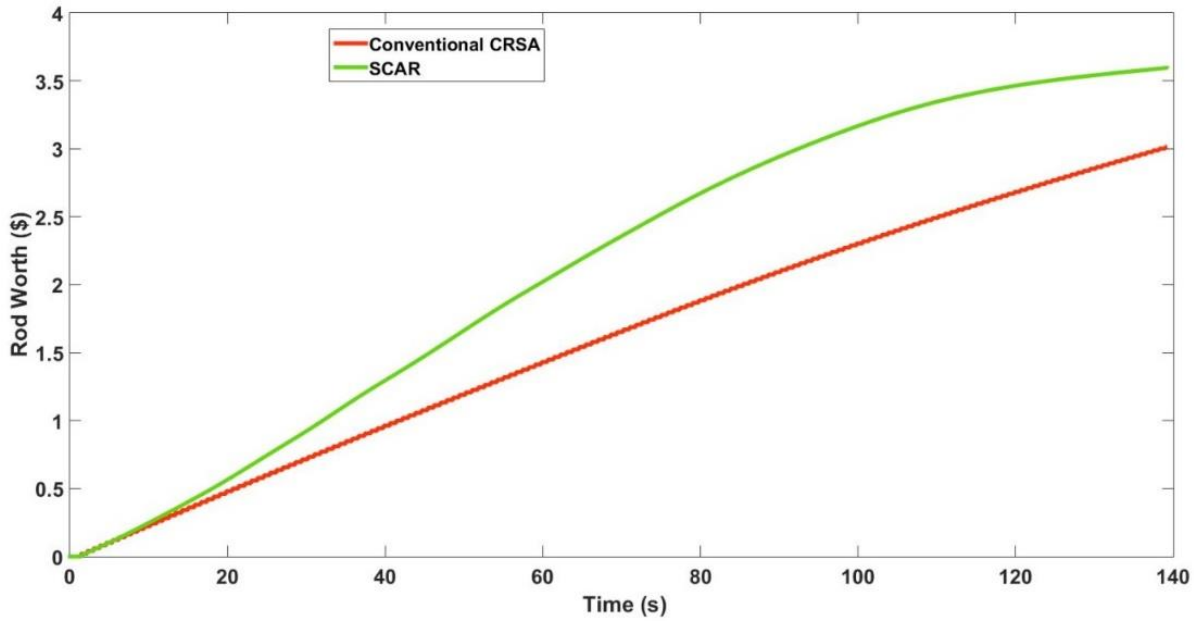

Figure 13. The simulation results of the reactivity worth value for conventional CRSA and SCAR.

In conventional CRSA, the conventional rod position algorithm with reactivity worth curve has been outlined with initial rod position 214 mm (10% FP) for all control rods (SH 214 mm =$1.779, SF 214 mm=$1.918, RG 214 mm =$2.653, TR 214 mm=$2.148) for the reactor at low power (critical) shown in Figure 12 [34]. For the SCAR algorithm, the reactivity worth curve is obtained at different initial rod positions, SF rod ($2.658) and SH rod ($2.430) at 284 mm, TR rod at 280 mm ($2.679) and RG rod at 100 mm ($0.73).

However, by referring to the control rod worth behaviour graph for RTP in [41], both conventional CRSA and SCAR have almost identical total of reactivity worth value which is $8.498. Total maximum reactivity worth value to fully lift-up all the control rods (at 381 mm) is about $13.144. Thus, the remaining reactivity is required to compensate for the power of the reactor. In conventional CRSA, four control rods are considered to be selected for reactivity insertion. In contrast, SCAR solely relies on the RG rod for the reactivity insertion thus no selection process is required.

The result between conventional CRSA and SCAR in obtaining the reactivity worth value is shown in Figure 13. The SCAR provided the most responsive reactivity compare to the conventional CRSA due to the high rate of reactivity inserted and reduced the complexity and time depending (delay time) on the selection rods in the nuclear reactor. The highest rod worth value, the more positive reactivity will be given to the reactor consequently the more power is produced. In addition, the SCAR can reduce switching time delays and time constants significantly in the actuators from moving four control rods to a single rod during the transient.

The application program for conventional CRSA and SCAR algorithm is developed using C/C++ language. This language is converted to MATLAB Simulink via computer simulation. For verification purposes based on experimental data, the program is written in C/C++ language is converted to NetArrays code (RTP Corp.) as shown in Figure 14 due to real-time hardware implementation using Distributed Control System (DCS).

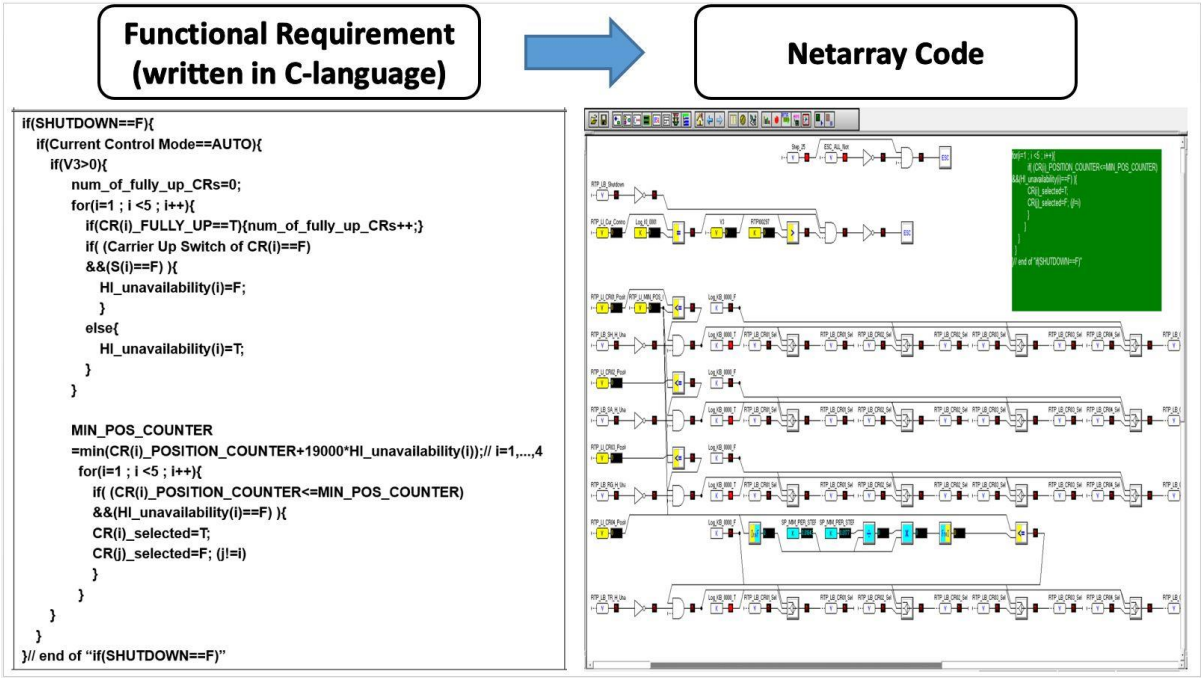

Figure 14. The converted process for conventional CRSA and SCAR algorithm using C/C++ language to NetArrays code for experimental setup approach.

To evaluate the performance of the proposed SCAR, the simulations and experimental data of the proposed FCA-SCAR is applied to load tracking where the pre-defined value is set as 1%. The performance of SCAR is compared with the FCA-conventional CRSA (FCA-CRSA) as shown in Figure 15. The safety parameter constraint is also included in the design of the controller. In this study, FCA using the same parameter constraint (23 steps per cycle for control rod speed) on the mechanical limits of the control rods as in [38]. Initial low power at 10% FP nominal core power.

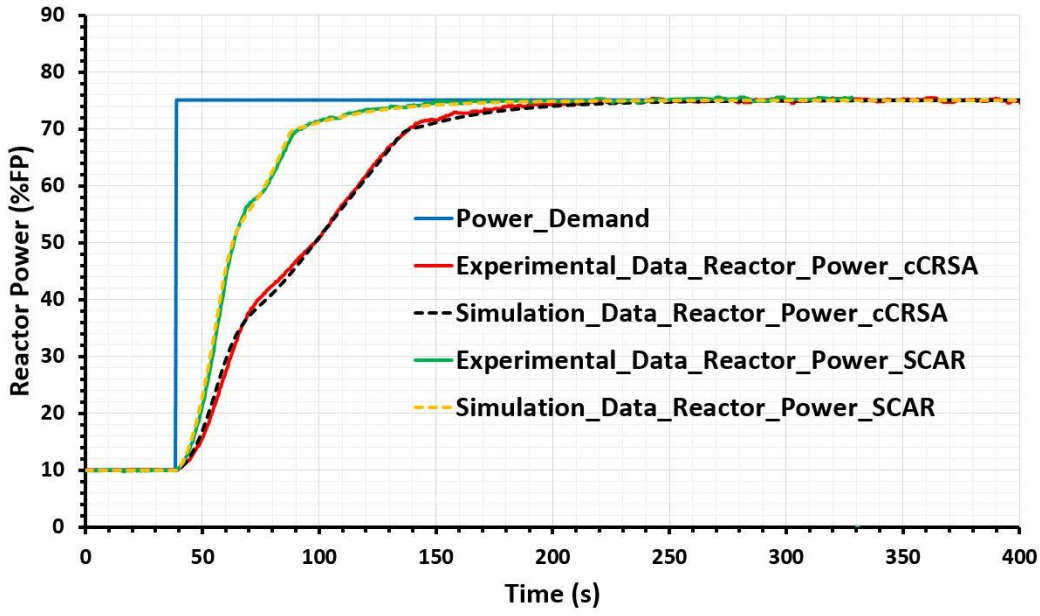

Figure 15. The power tracking performance using conventional CRSA (cCRSA) and SCAR via MATLAB Simulink simulation and experimental results.

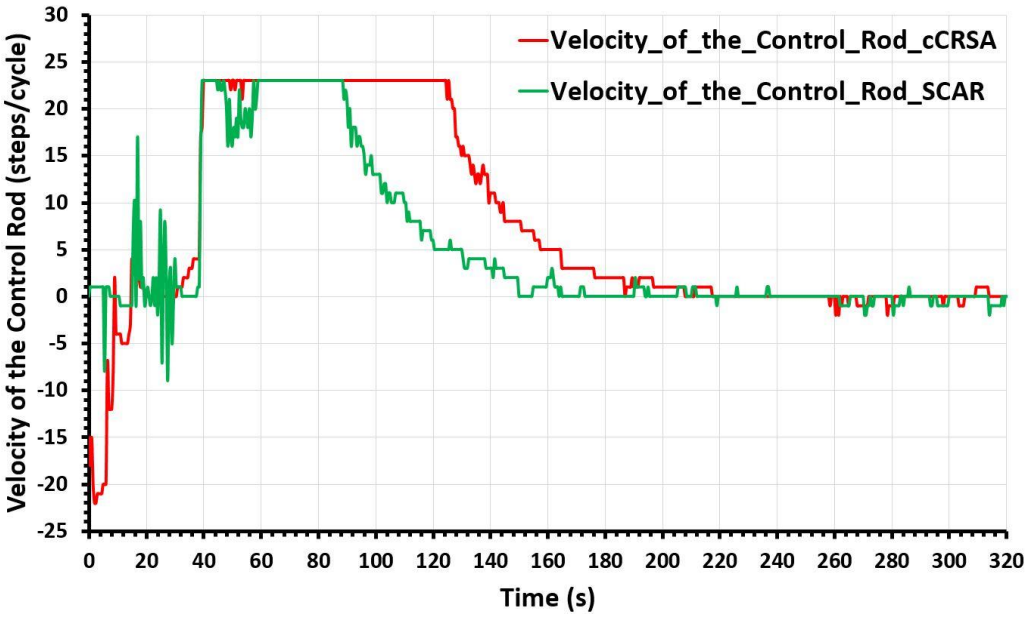

Figure 16. The experimental data for the velocity of the control rod using conventional CRSA (cCRSA) and SCAR.

Based on observation from Figure 15, FCA-SCAR ensures a stable power without causing the reactor to automatic trip. The result of SCAR shows a short rising time and the rate of power change less than the trip limit parameter (33.3%/s) [38]. However, small oscillations still can be observed at 60% FP due to the rate of power increment constraint by FCA.

Figure 16 shows the output signal of the FCA controller for velocity of the control rod, *V3*. From the experimental result obtained, the response from SCAR produced a good result in terms of reduced input actuation signal at CRDM. It is difficult to regulate control rods at low power 10%FP (0 s to 40 s) due to noisy conditions. However, both conventional CRSA and SCAR are good in eliminating the steady-state error and makes the reactor power output follow the power demand at steady-state. The SCAR used only one Regulating rod (the highest reactivity worth) to compensate the reactor power at steady-state whereas conventional CRSA used 4 rods. The conventional CRSA still can provide a better result with minimum chattering signal without fine-tuning at steady-state in a short time range; 200 s to 300 s in Figure 15 and presented in Table 1. Both CRSAs are not suffering from the chattering effect for a short time reactor operation. To capture the presence of switching imperfections such as switching time delays to select control rods and small time constants in the different actuators required long time operation more than 30 minutes based on previous data operation from RTP. The performance summary of conventional CRSA and SCAR at transient is tabulated in Table 2 quantitatively. The percentage of overshoot can be calculated using the equation in [12].

Table 1. Chattering error without fine-tuning in short time operation.

	Conventional CRSA	SCAR
Min (%)	74.6652	74.5447
Max (%)	75.4262	75.5322
Δe_{ce}	0.7610	0.9875

Table 2. Summary of performance of conventional CRSA and SCAR at 750kWth.

	Conventional CRSA	SCAR
Settling Time (T_s)	119.0 s	88.0 s
Percent Overshoot (%)	0.8316 %	0.7095%
Rise Time (T_r)	74.0 s	41.5 s

The workload on CRDM when to increase power level from 10% FP to 75% FP can be measured by the summation values of the velocity of the control rod (steps per cycle) from Figure 16. It can be verified in Table 3 that the SCAR with a large change in power demand can reduce the workload in small steps. The 3,176 steps workload is required within 280 s equal to 56.2152 mm which is the control rod distance travel for SCAR. The conventional SCAR takes long-distance about 87.1194 mm to perform the same task.

Table 3. The workload on CRDM (40s-320s).

	Conventional CRSA	SCAR
|Sum| *V3* (steps/cycle)	4922	3176

During steady-state, the SCAR will choose the lowest rod worth value of the control rod to move, the less positive or negative reactivity will be given to the reactor consequently the less power is produced or reduced at reactor core. As a result, it reduced the error power deviation (fluctuation power error) and the FCA controller can be minimized the control rod movement (reduced workload).

To evaluate the fine-tuning performance of the proposed SCAR, the experimental data of conventional CRSA is applied and started with four control rods. Then, the operation is continuous by reducing the number of control rods for fine-tuning at steady-state. The overall power control performance analysis is done using the gathered operation data for every 500 ms from RTP shown in Figure 17. The proposed SCAR compensates two or three control rods at steady-state in long time operation by freezing the highest rod worth value (RG rod) first. The current computer system checks if two or more control rods are frozen, the alarm dual control rod failure will be activated. For safety purposes, in the case of single rod failure and not solely depend only one rod to regulate reactor power at a steady-state region, two control rods; SF and SH rods which have about the same reactivity worth value will be needed for continuous operation. Figure 18 shows a closer view of chattering error at 75% FP between FCA-CRSA and FCA-SCAR during fine-tuning in a long-time operation. Overall, both CRSA are suffering from the chattering effect as expected within an acceptable range (±1% or 2%).

In order to reduce the chattering effect due to residual noise from neutron detector measurement and the presence of switching imperfections, the noise filter is used. From many types of noise filters, the moving average filter is selected as it is one of the favourable noise filters [45]. By referring to Figure 18, the fluctuation power error is higher without a filter for both conventional CRSA and SCAR thus hard to observe the data trends. However, with the increase in the number of moving average filters, slow changes in value are produced which allows easier data trend observation.

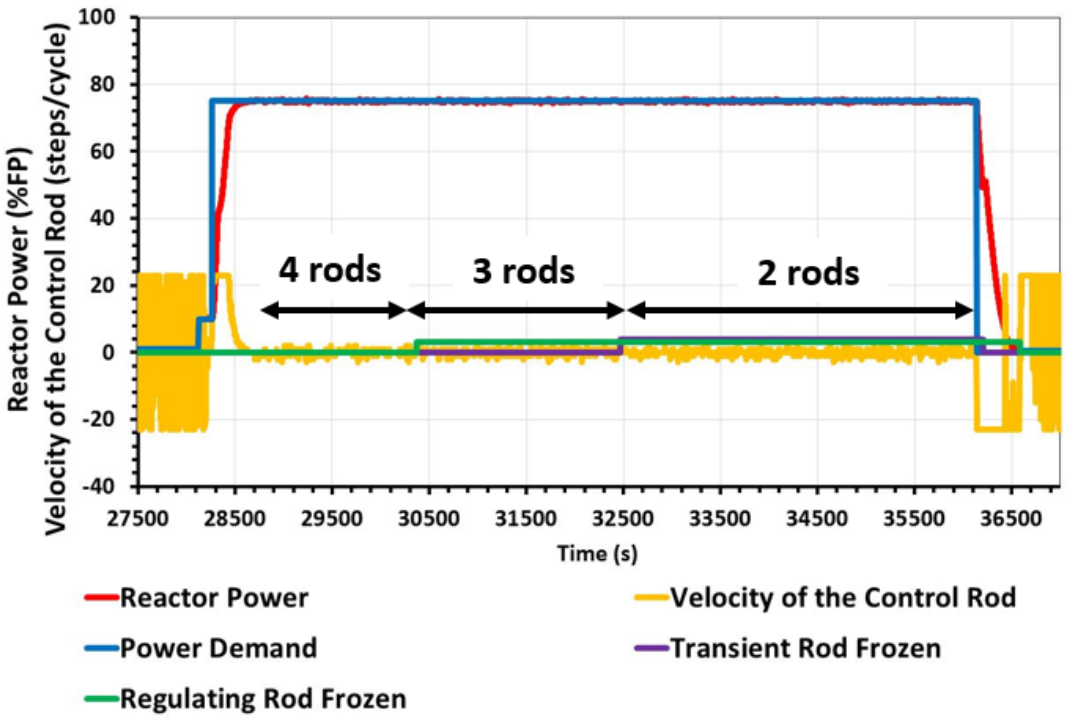

Figure 17. The fine-tuning performance at steady-state with different numbers of the control rod.

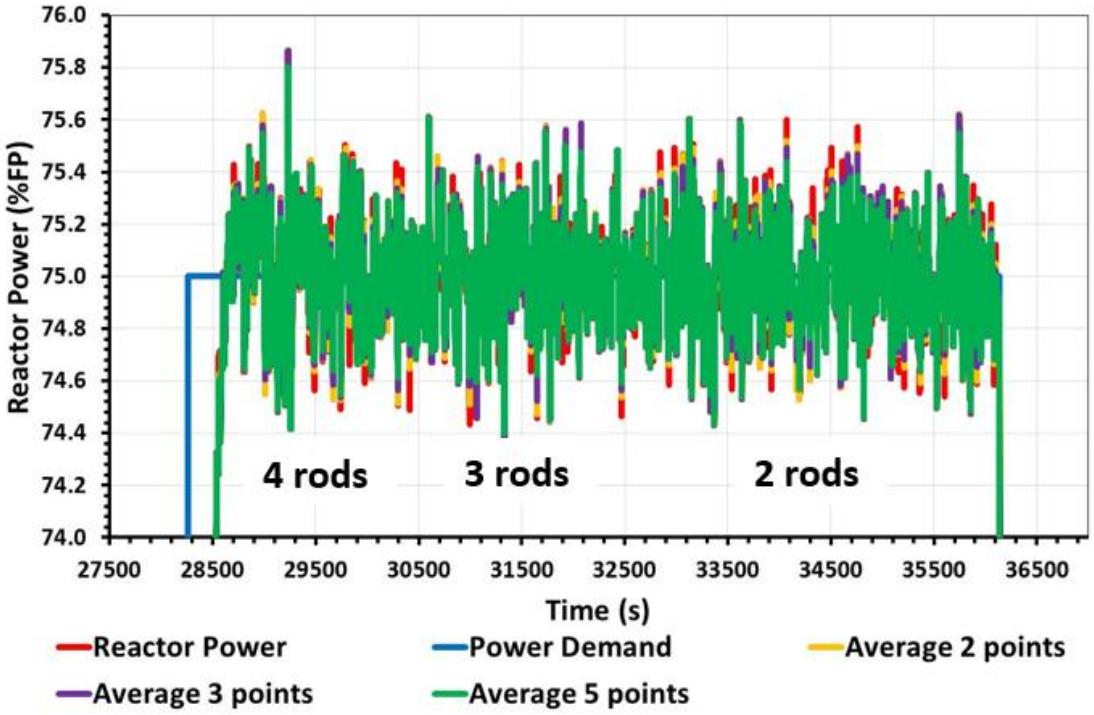

Figure 18. Comparison of fine-tuning performance at steady-state with different numbers of average point.

Table 4. Chattering error with fine-tuning during steady-state and with different numbers of average points.

	Conventional CRSA	SCAR	
	4 rods	3 rods	2 rods
Δe_{ce}	1.4498	1.2572	1.1898
Average 2 points, Δe_{ce}	1.4498	1.2572	1.1873
Average 3 points, Δe_{ce}	1.4498	1.2524	1.1865
Average 5 points, Δe_{ce}	1.4474	1.2061	1.1705

Table 4 presents the behaviour of using the different number of control rods for tuning at the high-power level. In overall, based on Table 2 to 4, the analysis shows that a SCAR offers generally better results than the conventional CRSA with the reduction in rise time up to 44%, workload up to 35%, settling time up to 26% and chattering error up to 18% of the nominal value. In addition, implementing a noise filter by taking a moving average can help in reducing the chattering error with the increase number of average points. However, a new SCAR design is not fully integrated (design separately) with the current controller and additional study is necessary in order to achieve the most effective SCAR for RTP.

CONCLUSIONS

The power tracking performance for a reactor can be improved by modifying the conventional Control Rod Selection Algorithm (CRSA). Instead of using four control rods, this paper proposed a Single Control Rod Algorithm (SCAR) that has less complexity and time response (delay time) for the selection of rods in the nuclear reactor. The proposed SCAR with FCA control strategy is useful for types of nuclear reactors have a big difference in control rod worth values to regulate reactor power by using the reactivity insertion control rod. With the utilization of SCAR, it is proved that the rise time, settling time, chattering and power fluctuation error can be reduced. Overall, the study is expected to significantly improve core power control at nuclear reactor by using SCAR to provide a fast response with reduced computational complexity, high accuracy and reduce overall operational cost through minimizing control rod drive damage. Future works include integrating the SCAR algorithm with the controller to reduce the complexity of the system, provide direct control and improved safety.

ACKNOWLEDGEMENTS

This work was supported by a Fundamental Research Grant Scheme (FRGS) grant (FRGS/1/2017/TK04/UTM/02/55, Vot No. 4F968) from the Ministry of Education, Malaysia. The author would like to thank all the individuals who have contributed in this paper especially to Dr Nurul Adilla Binti Mohd Subha from Universiti Teknologi Malaysia and to the Malaysian Nuclear Agency under Ministry of Energy, Science, Technology, Environment, and Climate Change, Malaysia (MESTECC) for the support.

REFERENCES

[1] Torabi M, Lashkari A, Masoudi SF, Bagheri S. Neutronic analysis of control rod effect on safety parameters in Tehran research reactor. Nuclear Engineering and Technology, 2018; 50(7): 1017–1023.

[2] Malaysia Nuclear Agency. Safety analysis report for PUSPATI TRIGA reactor. NUKLEARMALAYSIA/L/2014/12(S); 2014.

[3] Kim JH, Park SH, Na MG. Design of a model predictive load-following controller by discrete optimization of control rod speed for PWRs. Annals of Nuclear Energy, 2014; 71: 343–351.

[4] Lee YK, Lee JH, Kim HW, Kim SK, Kim JB. Drop performance test of conceptually designed control rod assembly for prototype generation iv sodium-cooled fast reactor. Nuclear Engineering and Technology, 2017; 49(4): 855–864.

[5] Shirazi SAM. The simulation of a model by SIMULINK of MATLAB for determining the best ranges for velocity and delay time of control rod movement in LWR reactors. Progress in Nuclear Energy, 2012; 54(1): 64–67.

[6] Badgujar KD. System science and control techniques for harnessing nuclear energy. Systems Science and Control Engineering, 2016; 4(1): 138–164.

[7] Andraws MS, Abd AA, Yousef AH, Mahmoud II, Hammad SA. Performance of receding horizon predictive controller for research reactor. In: 12th International Conference on Computer Engineering and System, Cairo, Egypt; 19-20 December, 2017.

[8] Coban R, Can B. A trajectory tracking genetic fuzzy logic controller for nuclear research reactors. Energy Conversion and Management, 2010; 51(3) 587–593.

[9] Kaiba T, Žerovnik G, Jazbec A, Štancar Ž, Barbot L, Fourmentel D, Snoj L. Validation of neutron flux redistribution factors in JSI TRIGA reactor due to control rod movements. Applied Radiation and Isotopes, 2015; 104: 34–42.

[10] Bhowmik PK, Dhar SK, Chakraborty S. Operation and control of TRIGA nuclear research reactor with PLC. International Journal of Information and Electronics Engineering, 2013; 3(6): 553–557.

[11] Coban R. A fuzzy controller design for nuclear research reactors using the particle swarm optimization algorithm. Nuclear Engineering and Design, 2011; 241(5): 1899–1908.

[12] Coban R. Power level control of the TRIGA Mark-II research reactor using the multifeedback layer neural network and the particle swarm optimization. Annals of Nuclear Energy, 2014; 69: 260–266.

[13] Borio Di Tigliole A, Cammi A, Gadan MA, Magrotti G, Memoli V. Study of a new automatic reactor power control for the TRIGA Mark II reactor at University of Pavia. In: 1st International Conference on Advancements in Nuclear Instrumentation, Measurement Methods and their Applications, Marseille, France; 7-10 June, 2009.

[14] Lee YJ. The control rod speed design for the nuclear reactor power control using optimal control theory. Journal of the Korean Nuclear Society, 1994; 26(4): 536–547.

[15] Edwards RM, Lee KY, Schultz MA. State feedback assisted classical control : an incremental approach to control modernization of existing and future nuclear reactors and power plants. Nuclear Technology, 1990; 92: 167–185.

[16] Edwards RM, Weng CK, Lindsay RW. Experimental development of power reactor advanced. In: 8th Power Plant Dynamics, Control and Testing Symposium, Tennessee, United States; 27-29 May, 1992.

[17] Suzuki K, Shimazaki J, Shinohara Y. Application of H∞ control theory to power control of a nonlinear reactor model. Nuclear Science and Engineering, 1993; 115: 142–151.

[18] Ansarifar GR, Rafiei M. Second-order sliding-mode control for a pressurized water nuclear reactor considering the xenon concentration feedback. Nuclear Engineering and Technology, 2015; 47(1): 94-101.

[19] Arab-Alibeik H, Setayeshi S. An adaptive-cost-function optimal controller design for a PWR nuclear reactor Annals of Nuclear Energy, 2003; 30(6): 739–754.

[20] Davijani NZ, Jahanfarnia G, Abharian AE. Nonlinear fractional sliding mode controller based on reduced order FNPK model for output power control of nuclear research reactors. IEEE Transactions on Nuclear Science, 2017; 64(1): 713–723.

[21] Edwards RM, Lee KY, Ray A. Robust optimal control of nuclear reactors and power plants. Nuclear Technology, 1991; 98(2): 137–148.

[22] Wang L, Wei X, Zhao F, Fu X. Modification and analysis of load follow control without boron adjustment for CPR1000. Annals of Nuclear Energy, 2014; 70: 317–328.

[23] Pérez-Cruz JH, Poznyak A. Automatic startup of nuclear reactors using differential neural networks. IFAC Proceeding Volumes, 2007; 40(20): 112–117.

[24] Rivero-Gutiérrez T, Benítez-Read JS, Segovia-De-Los-Ríos A, Longoria-Gándara LC, Palacios-Hernández JC. Design and implementation of a fuzzy controller for a TRIGA mark III reactor. Science and Technology of Nuclear Installations, 2012; 415805: 1-9.

[25] Ansarifar GR, Esteki MH, Arghand M. Sliding mode observer design for a PWR to estimate the xenon concentration & delayed neutrons precursor density based on the two point nuclear reactor model. Progress in Nuclear Energy, 2015; 79: 104–114.

[26] Cammi A, Ponciroli R, Borio Di Tigliole A, Magrotti G, Prata M, Chiesa D, Previtali E. A zero dimensional model for simulation of TRIGA Mark II dynamic response. Progress in Nuclear Energy, 2013; 68: 43–54.

[27] Pérez-cruz JH, Poznyak A. Design of a sliding mode neurocontroller for a nuclear research reactor. In: 8th International IFAC Symposium on Dynamics and Control of Process Systems, Cancún, Mexico; 4-6 June, 2007.

[28] Li G, Liang B, Wang X, Li X. Multivariable modeling and nonlinear coordination control of nuclear reactor cores with/without xenon oscillation using H∞ loop shaping approach. Annals of Nuclear Energy, 2018; 111: 82–100.

[29] Ravivarman R, Palaniradja K, Prabhu Sekar R. Performance enhancement of normal contact ratio gearing system through correction factor. Journal of Mechanical Engineering and Sciences, 2019; 13(3): 5242–5258.

[30] Eom M, Chwa D, Baang D. Robust disturbance observer-based feedback linearization control for a research reactor considering a power change rate constraint. IEEE Transactions on Nuclear Science, 2015; 62(3): 1301–1312

[31] Akin HL, Altin V. Rule-based fuzzy logic controller for a PWR-type nuclear power plant. IEEE Transactions on Nuclear Science, 1991; 38(2): 883–890.

[32] Rojas-Ramírez E, Benítez-Read JS, Segovia-De-Los Ríos A. A stable adaptive fuzzy control scheme for tracking an optimal power profile in a research nuclear reactor. Annals of Nuclear Energy, 2013; 58: 238–245.

[33] Shamseldin MA, Sallam M, Bassiuny AM, Abdel Ghany AM. Real-time implementation of an enhanced nonlinear PID controller based on harmony search for one-stage servomechanism system. Journal of Mechanical Engineering and Sciences, 2018; 12(4):4161–4179.

[34] Khoshahval F, Aziz A. Determination of the maximum speed of WWER-1000 nuclear reactor control rods. Annals of Nuclear Energy, 2016; 87(2): 58–68.

[35] Arab-Alibeik H, Setayeshi S. Improved temperature control of a PWR nuclear reactor using an LQG / LTR based controller. IEEE Transactions on Nuclear Science, 2003; 50(1): 211–218.

[36] Wang G, Wu J, Zeng B, Xu Z, Wu W, Ma X. Design of a model predictive control method for load tracking in nuclear power plants. Progress in Nuclear Energy, 2017; 101(B): 260–269.

[37] Chen CT. Linear System Theory and Design. 3rd ed. Oxford University Press, Inc; 1999.

[38] Minhat MS, Selamat H, Mohd Subha NA. Adaptive control method for core power control in TRIGA Mark II reactor. IOP Conference Series: Materials Science and Engineering, 2018; 298(012028): 1-15.

[39] Baang D, Suh Y, Kim SH. Power controller design and application to research reactor. In: Transactions of the Korean Nuclear Society Autumn Meeting, Gyeongju, Korea; 26-27 October, 2017.

[40] Baang D, Suh Y, Park C. Feedback power control for TRIGA-II research reactor. In: Transactions of the Korean Nucear Society Spring Meeting, Jeju, Korea; 18–19 May, 2017.

[41] Rabir MH, Jalal Bayar AM, Hamzah NS, Mustafa KA, Abdul Karim J, Mohamed Zin MR. RTP core measurement and simulation of thermal neutron flux distribution in the RTP core. IOP Conference Series: Materials Science and Engineering, 2018; 298(012029): 1–10.

[42] Malaysia Nuclear Agency. PUSPATI TRIGA reactor functional requirement for data acquisition and control system. Re-30-KJ-150-001; 2014.

[43] Qaiser SH, Bhatti AI, Iqbal M, Qadir J. System identification and robust Controller design for pool type research reactor. In: 13th IEEE IFAC International Conference on Methods Models in Automation and Robotics, Szczecin, Poland; 27-30 August; 2007.

[44] Do VD, Dang XK. The fuzzy particle swarm optimization algorithm design for dynamic positioning system under unexpected impacts. Journal of Mechanical Engineering and Sciences, 2019; 13(3): 5407–5423.

[45] Zhang Q, Hu Z, Deng B, Xu M, Guo Y. A simple iterative method for compensating the response delay of a self-powered neutron detector. Nuclear Science and Enginerring, 2017; 186(3): 1–10.